arXiv:1610.03058v1 [cond-mat.dis-nn] 10 Oct 2016

Intrinsic decoherence in isolated quantum systems

Yang-Le Wu, Dong-Ling Deng, Xiaopeng Li, and S. Das Sarma
Condensed Matter Theory Center and Joint Quantum Institute, Department of Physics, University of Maryland, College Park, MD 20742-4111, USA

(Dated: October 12, 2016)

We study the intrinsic, disorder-induced decoherence of an isolated quantum system under its own dynamics. Specifically, we investigate the characteristic timescale (i.e. the decoherence time) associated with an interacting many-body system losing the memory of its initial state. To characterize the erasure of the initial state memory, we define a new timescale, the intrinsic decoherence time, by thresholding the gradual decay of the disorder-averaged return probability. We demonstrate the system-size independence of the intrinsic decoherence time in different models, and we study its dependence on the disorder strength. We find that the intrinsic decoherence time increases monotonically as the disorder strength increases in accordance with the relaxation of locally measurable quantities. We investigate several interacting spin (e.g. Ising and Heisenberg) and fermion (e.g. Anderson and Aubry-André) models to obtain the intrinsic decoherence time as a function of disorder and interaction strength.

I. INTRODUCTION

Decoherence is an important issue in the practical realization of quantum computers, as it hinders the preservation and controlled manipulation of quantum information.[1] Combating decoherence in various quantum computing architectures has thus attracted a lot of attention from both theoretical and experimental communities in recent years. In this line of research, decoherence typically refers to the loss of quantum coherence in a system of controlled qubits due to the entanglement generated by inevitable couplings to the external environment. Significant efforts and progress have been made to reduce such couplings while maintaining the ability to reliably control the quantum system.[2–4]

In this paper we investigate a related, but distinct concept, the "intrinsic decoherence" in an *isolated* quantum system without any explicit coupling to the external environment. The decoherence here refers to the erasure of local quantum information in an initial non-eigenstate as the isolated system relaxes by itself (through interaction) to thermalization. This is motivated by the recent developments in the study of many-body localization,[5–12] where an interacting, isolated quantum system resists thermalization under strong disorder and retains indefinitely the quantum memory in its initial, highly excited state.[13,14] Here we take a closer look at the thermalization (or relaxation) dynamics in terms of both local observables and the global return probability. We aim to construct a quantitative measure of the gradual erasure of the initial state information during the time evolution of the isolated system, and study the dependence of the erasure rate on the disorder strength. The decoherence considered here arises from an intricate interplay between external noise (as manifested in the disorder) and interaction among all the qubits in the circuit, and is thus quite distinct from the corresponding purely environmental single-qubit decoherence considered in the context of quantum computing architectures. We use the word "decoherence" here in a loose qualitative manner (for example, "relaxation" rather than "decoherence" would have been an equally appropriate nomenclature here), but define the intrinsic decoherence time rather precisely (with respect to the initial state) so that there is no semantic confusion. The important point to be emphasized is that the intrinsic decoherence being studied here is a property of the *whole* interacting many-body system, and is not a single-qubit phenomenon.

We define a new quantity, dubbed the "intrinsic decoherence time", by thresholding the decay of the disorder-averaged return probability after a certain rescaling. This quantity captures the timescale over which the system loses track of the local information in the initial state under its own dynamics. We pay special attention to ensure that the intrinsic decoherence time thus defined is insensitive to finite-size effects and extrapolates properly to the thermodynamic limit.

We study this new quantity in four different models for both spins and interacting fermions. There is background disorder in all the models, and the models are, by definition, interacting models as each spin or fermion interacts with others. Across the different models, we consistently find that the intrinsic decoherence time increases monotonically as the disorder strength increases (presumably diverging in the many-body-localized systems where local initial state memory is preserved forever), and it only displays rather moderate dependence on system size with a reasonable scaling behavior. For comparison, we have also computed similar timescales extracted from local observables such as magnetization and density imbalance. We find that these timescales also exhibit similar monotonic dependence on disorder, giving confidence in the belief that the intrinsic decoherence time is an experimentally accessible physical property characterizing the relaxation dynamics of disordered interacting many-body systems.

The paper is organized as follows. In Sec. II we examine the dynamics of the disorder-averaged return probability in the transverse-field Ising model, and discuss the proper definition of the intrinsic decoherence time

based on the per-site return probability. We further characterize the intrinsic decoherence time in another three different models, namely, the nearest-neighbor Heisenberg model with a random magnetic field in Sec. III, the Anderson model of the interacting fermions with a random on-site potential in Sec. IV, and also the interacting Aubry-André incommensurate model in Sec. V. We conclude the paper in Sec. VI.

II. INTRINSIC DECOHERENCE IN TRANSVERSE-FIELD ISING MODEL

We aim to characterize the intrinsic decoherence in an isolated, disordered quantum system. As a specific example, we consider a linear array of coupled trapped-ion qubits, described by the disordered transverse-field Ising model[10,15]

$$H_{\rm Ising} = \sum_{i<j} J_{i,j}\sigma_i^x\sigma_j^x + \frac{1}{2}\sum_i h_i\sigma_i^z. \tag{1}$$

With some minor modifications, the same Hamiltonian, in principle, applies also to the capacitively-coupled singlet-triplet semiconductor spin qubits. The inter-qubit couplings take the power-law form $J_{i,j} = J_0/|i-j|^\alpha$, while the transverse fields h_i are drawn uniformly from $[h_0 - W, h_0 + W]$. For simplicity, we work in the short-range coupled regime and pick $\alpha = 3.0$ and $h_0 = 4J_0$. This model has recently been experimentally demonstrated to exhibit features of many-body localization for disorder W stronger than a few J_0.[10,16]

We prepare the coupled qubits in the Néel initial state $|\psi(0)\rangle = |\uparrow\downarrow\cdots\uparrow\downarrow\rangle$ and track their time evolution. We define the disorder-averaged return probability to the initial state as

$$R(t) = \left[\!\!\left[\left|\langle\psi(t)|\psi(0)\rangle\right|^2 \right]\!\!\right], \tag{2}$$

where the double brackets $[\![\cdot]\!]$ denote averaging over disorder realizations. For the results presented in this paper, we typically average over 10^3 disorder samples for each parameter set. Obviously, the dynamics of the return probability depends both on the Hamiltonian and the initial state (chosen to be the standard Néel state here).

Figure 1 shows the time dependence of the disorder-averaged return probability $R(t)$ for $N = 2$ and 8 qubits under various strengths of disorder. For $N = 2$, we observe a persistent oscillation of $R(t)$ with a decaying envelope. Mathematically this is reminiscent of (although physically different from) the damped Rabi oscillations of a single qubit due to couplings to the external environment. Naively, one may try to extract a decoherence timescale from the decaying envelope in the same spirit as the relaxation time T_1 obtained from Rabi oscillations.[3] Unfortunately, this intuitive picture of a damped oscillator breaks down once the system grows beyond a couple of qubits, and no such simple analogy to Rabi oscillations or noninteracting single qubit systems is possible

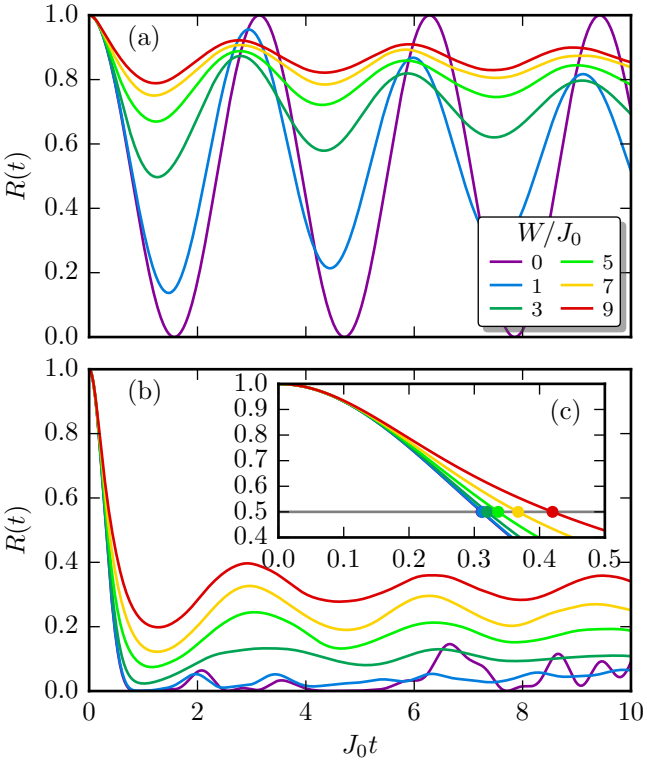

FIG. 1. Dynamics of the disorder-averaged return probability $R(t)$ for (a) $N = 2$ and (b) $N = 8$ Ising qubits for various disorder strengths W. The inset (c) illustrates the thresholding procedure that defines T. The three panels share the same color code illustrated in (a).

in the multiqubit situation. In Fig. 1(b), we find that for $N = 8$ qubits, the disorder-averaged return probability $R(t)$ does not exhibit a gradual decay of oscillations. Instead, $R(t)$ undergoes a monotonic, steep decline followed by weak irregular oscillations with no clear decay envelope. In other words, when the disordered quantum system has a large enough Hilbert space, we find that the erasure of the initial state information occurs mostly at the beginning of the time evolution.

This motivates us to depart from the usual approach of characterizing the decaying envelope, and instead focus on the monotonic decline of $R(t)$ at the beginning. To this end, we impose an (arbitrary) threshold R_0 on $R(t)$ and define an "effective decoherence time" T as the moment when $R(t)$ drops below R_0 for the first time,

$$T = \min\{t : R(t) < R_0\}. \tag{3}$$

Figure 1(c) illustrates the thresholding procedure using $R_0 = 0.5$ on the $N = 8$ data as an example. Changing the threshold R_0 will change the absolute scale for T without affecting any of its qualitative behavior (which we have checked explicitly).

The quantity T defined above characterizes the time needed for the isolated system to relax from the initial state, and it may serve as a characteristic timescale for

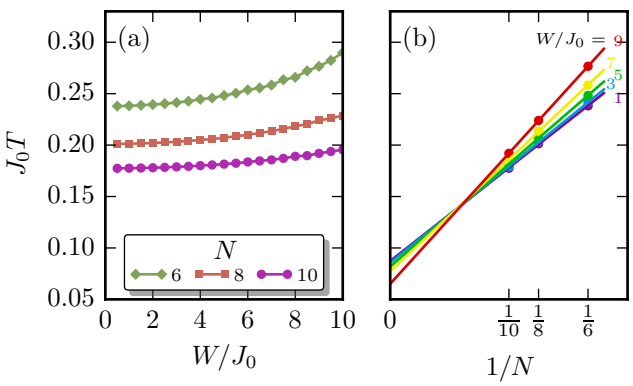

FIG. 2. Dependence of the timescale T extracted from the disorder-averaged return probability $R(t)$ on (a) the disorder strength W and (b) the system size N of the Ising model, with threshold $R_0 = 0.75$. The lines in (a) are guide to the eye, while those in (b) are linear fits of the data points grouped by W.

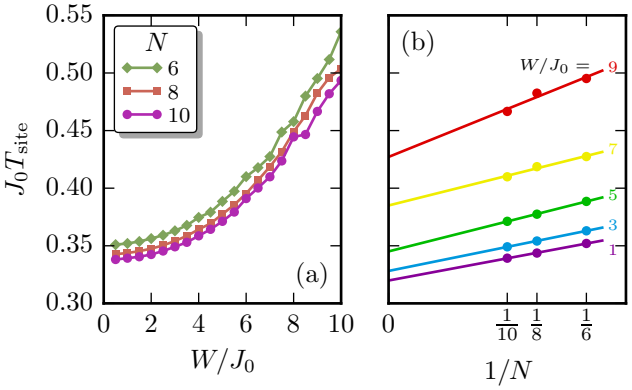

FIG. 3. Dependence of the intrinsic decoherence time $T_{\rm site}$ extracted from the disorder-averaged per-site return probability $R_{\rm site}(t)$ on (a) the disorder strength W and (b) the system size N of the Ising model, with threshold $R_0 = 0.9$. The lines in (a) are guide to the eye, while those in (b) are linear fits of the data points grouped by the disorder strength W.

such intrinsic decoherence. In Fig. 2, we examine the dependence of T on the disorder strength W for various system sizes N. We observe that T slightly increases as disorder W increases, consistent with the intuition that a strong disorder impedes thermalization and induces localization. However, we also find that T suffers from a severe system-size dependence, dropping sharply as the number of qubits N increases. The size dependence completely eclipses the variation of T as the disorder strength W changes. From the linear extrapolation in Fig. 2(b), even the qualitative trend of the W dependence of T may shift from increasing to decreasing when the system size is large enough. It therefore appears that although T seems to be a reasonable quantity, its use as an effective system decoherence time is fraught with the pitfalls of severe finite size effects.

Such an undesirable behavior of T is rooted in its definition based on thresholding the return probability. For a many-qubit system, the return probability has a strong system-size dependence from the dilution effect in the exponentially large Hilbert space. As the system size N increases, the fixed threshold R_0 on the disorder-averaged return probability becomes effectively easier to reach. Thus, the effective decoherence time T for the whole system turns out to be a poor definition or characterization for intrinsic decoherence because of uncontrolled finite size effects, although it may very well work for a system with finite and fixed number of qubits.

To get around the system-size dependence, we now introduce the "per-site" return probability for a system of N qubits by taking the N-th root of the usual return probability, and define its disorder average as

$$R_{\rm site}(t) = \left[\!\!\left[\left| \langle\psi(t)|\psi(0)\rangle \right|^{2/N} \right]\!\!\right] . \tag{4}$$

Here, the N-th root effectively folds the exponentially large Hilbert space of N qubits so that $R_{\rm site}(t)$ behaves like the effective fidelity of a single qubit. This rescaling can also be understood in a spirit similar to the per-site error in density-matrix-renormalization-group calculations.[17] Using the rescaled return probability, we define the intrinsic decoherence time

$$T_{\rm site} = \min\{t : R_{\rm site}(t) < R_0\} \tag{5}$$

as the time when $R_{\rm site}(t)$ drops below a given threshold R_0 for the first time.

In Fig. 3(a) we find that the intrinsic decoherence time $T_{\rm site}$ increases with the disorder strength W because relaxation or thermalization of the many-body system is slowing down with increasing disorder. Further, the data for different system sizes almost collapse into a single curve. The residual system-size dependence is more clearly visible in Fig. 3(b). We find that $T_{\rm site}$ has an approximately linear dependence on the inverse system size $1/N$, and the slope of this dependence does not change significantly as disorder W changes. It should be noted that varying the threshold R_0 affects the precise value of $T_{\rm site}$, but does not introduce any qualitative change to its dependence on disorder or system size. Hence, the intrinsic decoherence time $T_{\rm site}$ defined in Eq. (5) provides a system-size insensitive universal measure of the rate at which an isolated quantum system loses its memory of the collective initial state.

Despite the rescaling, $T_{\rm site}$ is still defined from a global quantity that cannot be measured locally. It is thus instructive to compare the behavior of $T_{\rm site}$ with the corresponding decay time of local observables. As a specific example, we compute the dynamics of the normalized Hamming distance.[10,18] For the Néel initial state that we consider, the disorder average of the Hamming distance is simply given by

$$\mathcal{D}(t) = \frac{1}{2} - \frac{1}{2N} \sum_j^N (-1)^j \left[\!\!\left[\langle\psi(t)|\sigma_j^z|\psi(t)\rangle \right]\!\!\right] . \tag{6}$$

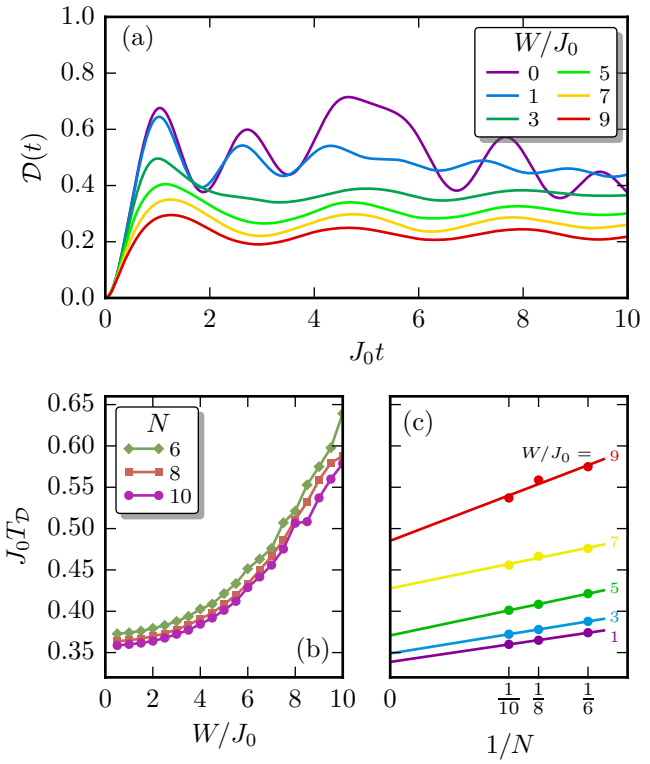

FIG. 4. (a) Dynamics of the Hamming distance from the initial Néel state of the Ising spins. Dependence of the intrinsic decoherence time $T_\mathcal{D}$ extracted from the disorder-averaged Hamming distance $\mathcal{D}(t)$ on (b) the disorder strength W and (c) the system size N, with threshold $\mathcal{D}_0 = 0.25$. The lines in (b) are guide to the eye, while those in (c) are linear fits of the data points grouped by the disorder strength W.

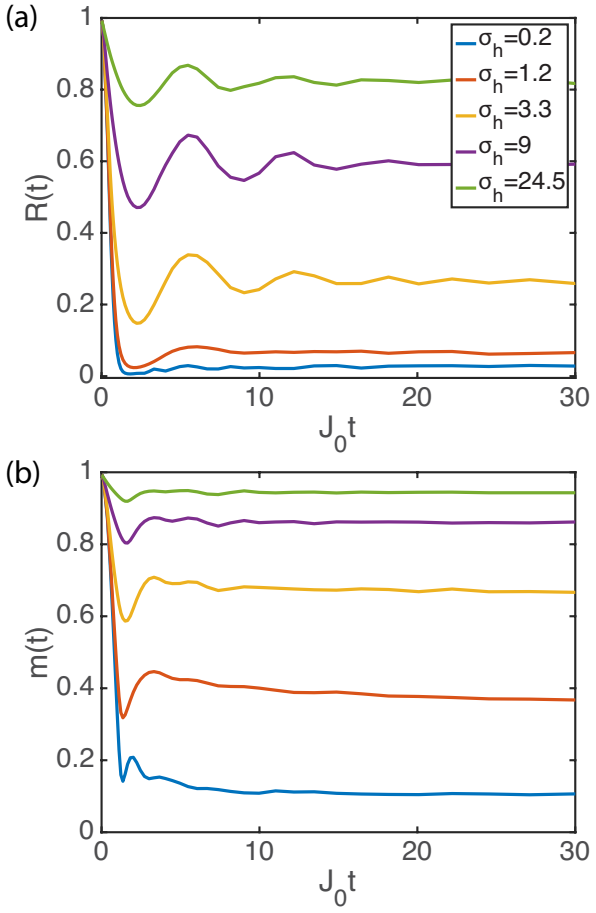

FIG. 5. Dynamics of (a) the return probability and (b) the local magnetization for the Heisenberg model with $N = 12$ spins, $\sigma_J = 0.1J_0$, and different disorder strengths σ_h. (a) and (b) share the same legend.

Figure 4(a) shows the time dependence of $\mathcal{D}(t)$ for various strengths of disorder W. We find that the dynamics of $\mathcal{D}(t)$ consists of an initial stage of monotonic increase followed by weak but irregular oscillations. Similar to the handling of the return probability $R(t)$, we can define another measure of the intrinsic decoherence by thresholding $\mathcal{D}(t)$,

$$T_\mathcal{D} = \min\{t : \mathcal{D}(t) > \mathcal{D}_0\}. \tag{7}$$

Figure 4(b) and (c) show the dependence of this alternative measure on the disorder strength as well as the system size. Similar to $T_{\rm site}$, here we find that $T_\mathcal{D}$ also increases with the disorder strength W and is largely insensitive to system size. This consistency between the decoherence timescales extracted from the per-site return probability and from local observables lends further support to our procedure of quantifying the intrinsic decoherence time.

In the rest of this paper, we provide further characterizations of the intrinsic decoherence time in three additional models, namely the Heisenberg model, the interacting Anderson model, and the interacting Aubry-André model. Throughout we use the definition of intrinsic decoherence time $T_{\rm site}$ as defined and discussed above on a per-site basis in order to eliminate finite size effects.

III. HEISENBERG MODEL

In this section, we study the intrinsic decoherence time in the Heisenberg model. We consider an 1D array of N quantum dots each hosting one localized electron.[19,20] This model is the appropriate description for the so-called exchange-gate architectures in semiconductor spin quantum computation, with the neighboring dots coupled through an exchange coupling arising from the combination of inter-dot Coulomb interaction and the single-particle inter-dot wavefunction overlap.[21–23] The collective dynamics of the coupled spin qubits under a local magnetic field is described by the following Heisenberg Hamiltonian,[24]

$$H = \sum_{k=1}^{N} J_k \mathbf{S}_k \cdot \mathbf{S}_{k+1} + \sum_{k=1}^{N} h_k S_k^z. \tag{8}$$

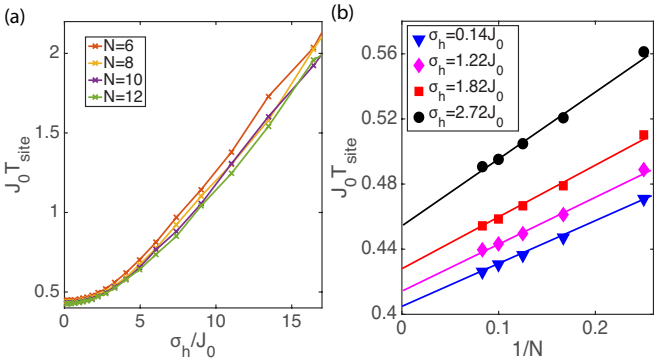

FIG. 6. (a) Intrinsic decoherence time determined from the per-site return probability (defined in Eq.5), as a function of increasing Overhauser noise strength σ_h, for the Heisenberg model with different system sizes. (b) System-size dependence of $T_{\rm site}$ for different σ_h. The lines in (b) are linear fits of the data. Here, we have fixed $\sigma_J = 0.1J_0$ and the threshold value is $R_0 = 0.95$.

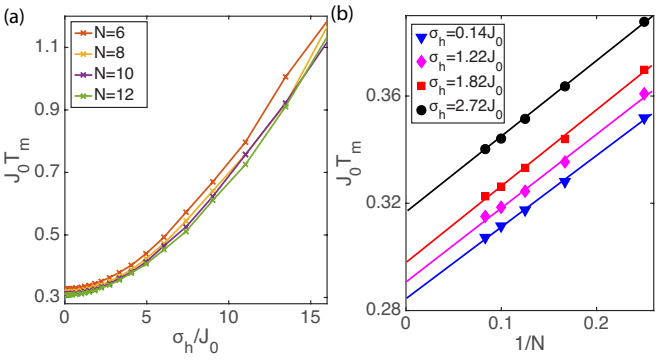

FIG. 7. (a) Intrinsic decoherence time determined from the local magnetization $m(t)$, as a function of increasing Overhauser noise strength σ_h, for the Heisenberg model with different system sizes. (b) System-size dependence of T_m for different σ_h. The lines are linear fits of the data. Here, the threshold value is chosen to be $m_0 = 0.9$ and we have fixed $\sigma_J = 0.1J_0$.

Here, the local magnetic field h_k and the exchange coupling J_k are independent random variables drawn from the normal distributions $\mathcal{N}(0, \sigma_h^2)$ and $\mathcal{N}(J_0, \sigma_J^2)$, respectively. The standard deviations σ_h and σ_J describe the strengths of Overhauser and charge noise,[25] respectively, with the Overhauser noise being a measure of the background fluctuations in the local magnetic field at the qubits (which could arise, for example, from the very slow nuclear fluctuations whose dynamics is being ignored here). The total spin $S^z = \sum_k S_k^z$ is conserved, and we focus only on the $S^z = 0$ sector to simplify the calculation. We truncate the charge noise distribution to the region $J_k > 0$ since the quantum dot exchange couplings are typically positive.[24]

Similar to the previous section on trapped-ion qubits, here we also consider the antiferromagnetic Néel initial state $|\psi(0)\rangle = |\uparrow\downarrow\cdots\uparrow\downarrow\rangle$ and track the time evolution $|\psi(t)\rangle = e^{-iHt}|\psi(0)\rangle$. We calculate the disorder-averaged return probability $R(t)$ [see Eq. (2)] and the local magnetization $m(t)$ commonly studied in the many-body-localization literature,[7,8,14]

$$m(t) = \left[\!\!\left[\frac{1}{N}\sum_k \left| \langle\psi(t)|\sigma_k^z|\psi(t)\rangle \right| \right]\!\!\right], \qquad (9)$$

where $\sigma_k^z = 2S_k^z$ is the usual Pauli-Z matrix. In this section, the number of random realizations used ranges from 10^4 for $L = 4$ to 10^3 for $L = 12$.

In Fig. 5, we plot the time dependence of the return probability (Fig. 5a) and the local magnetization (Fig. 5b) for $N = 12$. We find that for small σ_h, both the return probability and the local magnetization decay quickly, while for large σ_h, they first decrease a little bit and then remain stable at some finite value. This can be understood from the many-body localization-delocalization perspective.[14] For small σ_h, the system is in an extended delocalized phase and thermalizes quickly, leading to the fast decay of $R(t)$ and $m(t)$. In the thermodynamic limit $L \to \infty$, both $R(t)$ and $m(t)$ eventually vanish at large t. On the other hand, by increasing σ_h, the system will eventually go through a many-body-localization transition into a localized phase at some large critical disorder. In the localized region, the dynamics is drastically suppressed and certain local information is preserved even in the infinite time limit. Thus, in this localized large-disorder region, $R(t)$ and $m(t)$ first decay a little bit (mainly due to the wave-packet expansion within the localization length) and then remain stable at a finite value for a finite system size because of memory retention in the many body localized state. In this large-disorder localized phase the effective decoherence time then becomes infinite in the thermodynamic limit as the system simply fails to thermalize.

We now turn to the study of the intrinsic decoherence time. We first focus on the case of return probability. As discussed in the previous section, we can extract the intrinsic decoherence time $T_{\rm site}$ [see Eq. (5)] from the per-site return probability. In Fig. 6(a), we find that the calculated intrinsic decoherence time increases with increasing Overhauser noise strength σ_h, as expected from the localization physics. Fig. 6(b) shows the system-size dependence of the extracted $T_{\rm site}$. Similar to the transverse-field Ising model, an approximately linear dependence of $T_{\rm site}$ on the inverse system size $1/N$ is obtained for each fixed σ_h. Moreover, the slope of the linear dependence does not vary much as σ_h varies. This strong suppression of finite-size effect again explicitly shows the advantage of defining the intrinsic decoherence time based on per-site return probability.

As shown in Fig. 5(b), we have also computed the dynamics of the local magnetization $m(t)$ for different disorder strengths σ_h. Similar to $T_{\rm site}$ defined in the previous section, we can construct another measure of the intrinsic

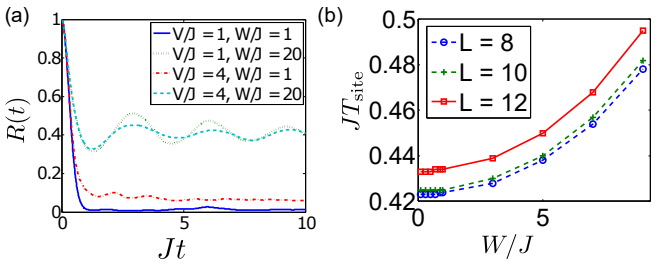

FIG. 8. Disorder-averaged dynamics of the return probability and the corresponding decoherence time for the interacting Anderson model. We choose initial states with fermions occupying random lattice sites. (a) shows the dynamical evolution of the return probability $R(t)$ for different interaction V/J and disorder strengths W/J. We average over 10^3 disorder realizations with one random initial state for each realization. (b) shows the intrinsic decoherence time $T_{\rm site}$ (Eq. (5)) with the threshold $R_0 = 0.9$. In (b), the interaction strength is fixed to be $V/J = 1$. Using different interaction strengths does not change the qualitative features shown here.

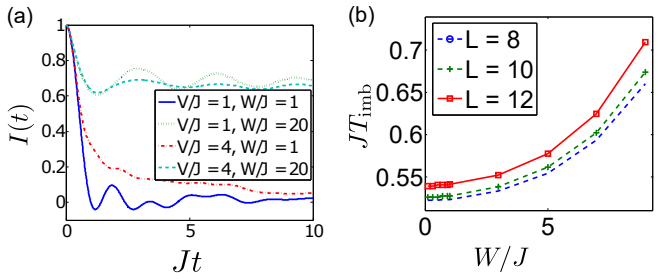

FIG. 9. Disorder-averaged dynamics of the number imbalance and the corresponding relaxation time for the interacting Anderson model. We choose initial states with fermions occupying random sites. (a) shows the dynamics of the disorder-averaged number imbalance $I(t)$ for different interaction V/J and disorder strengths W/J. We average over 10^3 disorder realizations with one random initial state in each realization. (b) shows the decoherence time $T_{\rm imb}$ as determined by the time $I(t)$ decays to the threshold $I_0 = 0.5$. In (b) the interaction strength is fixed to be V/J =1.

decoherence by thresholding $m(t)$,

$$T_m = \min\{t : m(t) < m_0\}. \tag{10}$$

Fig. 7(a) shows the dependence of T_m on the Overhauser strength σ_h. We find again that the such-defined intrinsic decoherence time increases with increasing σ_h. In addition, the data for different system sizes collapse approximately into a single curve, manifesting an apparent scaling behavior. The residual system-size dependence of T_m is shown in Fig. 7(a). Similar to the case of $T_{\rm site}$, we find that T_m has a linear dependence on $1/N$ and the slope of the dependence does not change significantly as σ_h changes.

IV. INTERACTING ANDERSON MODEL

As another example, in this section we study intrinsic decoherence in the interacting Anderson model,

$$H = \sum_i -J[c_i^\dagger c_{i+1} + c_{i+1}^\dagger c_i] + h_i c_i^\dagger c_i + V\sum_i c_i^\dagger c_{i+1}^\dagger c_{i+1} c_i. \tag{11}$$

Here J is the tunneling strength and V is the interaction strength between nearest neighbors. The random potential h_i is drawn uniformly from $[-W/2, W/2]$. We focus on half filling for the interacting Anderson model. This model has been widely studied in the context of many-body localization.[5,6,26–30] With the interaction strength $V/J = 2$, the model reduces to the Heisenberg model in Eq. (8) with $\sigma_J = 0$.

We calculate the relaxation dynamics of the disorder-averaged return probability and the number imbalance[9] relaxation for initial product states with particles occupying random lattice sites. Note that this choice is different from the Néel states used for spin models. The average number imbalance is defined by

$$I(t) = \left[\!\!\left[\frac{N_1(t) - N_0(t)}{N_1(t) + N_0(t)} \right]\!\!\right], \tag{12}$$

with N_1 (N_0) referring to the particle number in the initially occupied (unoccupied) sites,[31] and the double brackets $[\![\cdot]\!]$ now denoting an average over both disorder realizations and initial state configurations. The dynamical evolution of the return probability and the corresponding decoherence time are shown in Fig. 8. The number imbalance dynamics and its decoherence time $T_{\rm imb}$ are shown in Fig. 9, with $T_{\rm imb}$ defined by thresholding $I(t)$ in a similar fashion to Eq. (10).

When the disorder W is weak, both the return probability and the number imbalance decay quickly to almost zero, indicating a fast memory loss in the thermal phase. The intrinsic decoherence times determined from the return probability and the number imbalance qualitatively agree with each other. Both of them increase monotonically as we increase the disorder strength. In contrast, when the system is in a many-body localized phase at strong disorder, the number imbalance and the per-site return probability remain finite even in the long time limit. The corresponding monotonic increase of the decoherence time with increasing disorder strength provides a quantitative characterization of the memory retention protected by localization.

Compared with the two spin models, we find that the interacting Anderson model has a slightly stronger finite size effect. This is manifested in the scaling of both $T_{\rm site}$ determined from the return probability and $T_{\rm imb}$ determined from the number imbalance.

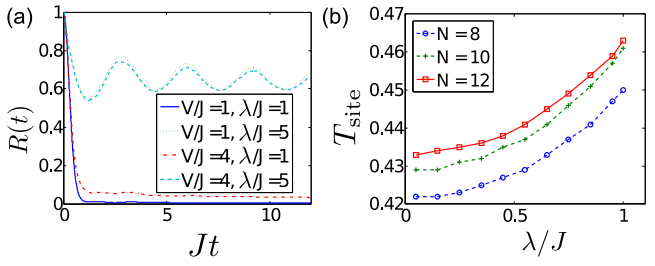

FIG. 10. Dynamics of the return probability and the corresponding decoherence time for the interacting Aubry-André model. In the initial state, fermions occupy random lattice sites. (a) shows the dynamical evolution of the return probability $R(t)$ for different interaction V/J and incommensurate lattice potential strengths λ/J. We average over 10^3 different ϕ-realizations (Eq. (13)). (b) shows the intrinsic decoherence time $T_{\rm site}$ (Eq. (5)) with the threshold $R_0 = 0.9$. In (b), the interaction strength is fixed to be $V/J = 1$.

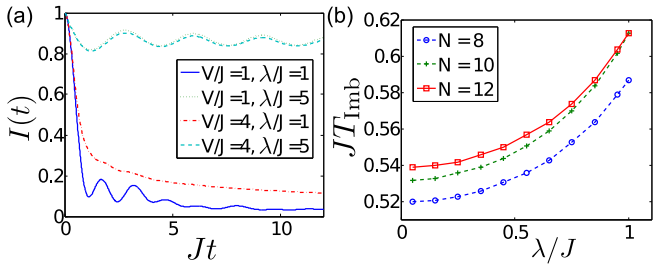

FIG. 11. The number imbalance dynamics and the corresponding relaxation time for the interacting Aubry-André model. (a) shows the dynamics of the number imbalance $I(t)$ with varying interaction V/J and incommensurate potential strengths λ/J. We average over 10^3 different ϕ-realizations with one random initial state (fermions occupying random sites) in each realization. (b) shows the decoherence time $T_{\rm imb}$ as determined by the time $I(t)$ decays to the threshold $I_0 = 0.5$. In (b) the interaction strength is fixed to be V/J =1.

V. INTERACTING AUBRY-ANDRÉ MODEL

In this section, we study the decoherence for the interacting Aubry-André model.[28,32–37] This model can be defined by replacing the random potential h_j in Eq. (11) with an incommensurate lattice potential

$$h_j = 2\lambda \cos(2\pi Q j + \phi), \tag{13}$$

where Q is an irrational number, here chosen to be the golden ratio.

In parallel with the interacting Anderson model, we have calculated the dynamics of the return probability and the number imbalance for the Aubry-André model following initial states with fermions occupying random sites. As shown in Figs. 10 and 11, the numerical data are qualitatively similar to those of the Anderson model, except with a slightly stronger finite size effect. We still find a monotonic dependence of the decoherence times on the disorder strength.

VI. CONCLUSION

In this paper we have studied the intrinsic decoherence in the time evolution of an isolated quantum system due to disorder. We analyze the scaling of the return probability as a function of system size, and propose a quantitative, system-size insensitive measure for the erasure of the initial state memory. We call this measure the intrinsic decoherence time of the isolated quantum system. Using four different models, we characterize the dependence of the intrinsic decoherence time on both the system size and the disorder strength, and we compare it with other timescales in the relaxation of local observables. We find that our definition of the intrinsic decoherence time consistently captures the timescale associated with the initial state memory retention, and it increases monotonically as the system becomes more disordered. Our results introduce new quantitative measures on how fast an isolated disordered system forgets its initial state information, and may provide useful guidance for future experiments. In particular, experiments in cold atomic gases and ion traps could mimic our results for the Anderson model and the Ising model respectively, whereas our Heisenberg model results can be compared eventually with multiqubit quantum dot based semiconductor spin qubit systems.

We emphasize that the intrinsic decoherence time studied theoretically in our work is a physical measure characterizing the loss of memory in disordered quantum interacting systems, which should be directly accessible in experiments through the measurement of time-dependent magnetization (or number imbalance). Our work can thus be used for a quantitative study of many-body localization and decoherence phenomena of wide interest. We also emphasize that the precise value of the intrinsic decoherence time would depend not only on the system Hamiltonian, but also on the starting initial state which must be a non-eigenstate of the Hamiltonian. We have used reasonable physical initial states (e.g. Néel states for our Ising and Heisenberg studies) because these are easy to prepare in the laboratory, but the qualitative behavior of the intrinsic decoherence time should not depend on the precise choice of the initial state (or the precise thresholding procedure) as long as the system starts in a generic unentangled product state.

ACKNOWLEDGMENT

This work is supported by JQI-NSF-PFC and LPS-MPO-CMTC. We acknowledge the University of Maryland supercomputing resources (http://www.it.umd.edu/hpcc) made available in conducting the research reported in this paper.

[1] D. P. DiVincenzo, Fortschritte der Physik **48**, 771 (2000).
[2] T. D. Ladd, F. Jelezko, R. Laflamme, Y. Nakamura, C. Monroe, and J. L. O'Brien, Nature **464**, 45 (2010).
[3] F. A. Zwanenburg, A. S. Dzurak, A. Morello, M. Y. Simmons, L. C. L. Hollenberg, G. Klimeck, S. Rogge, S. N. Coppersmith, and M. A. Eriksson, Rev. Mod. Phys. **85**, 961 (2013).
[4] M. H. Devoret and R. J. Schoelkopf, Science **339**, 1169 (2013).
[5] D. M. Basko, I. L. Aleiner, and B. L. Altshuler, Annals of Physics **321**, 1126 (2006).
[6] V. Oganesyan and D. A. Huse, Phys. Rev. B **75**, 155111 (2007).
[7] A. Pal and D. A. Huse, Phys. Rev. B **82**, 174411 (2010).
[8] J. Z. Imbrie, Journal of Statistical Physics **163**, 998 (2016).
[9] M. Schreiber, S. S. Hodgman, P. Bordia, H. P. Lüschen, M. H. Fischer, R. Vosk, E. Altman, U. Schneider, and I. Bloch, Science **349**, 842 (2015).
[10] J. Smith, A. Lee, P. Richerme, B. Neyenhuis, P. W. Hess, P. Hauke, M. Heyl, D. A. Huse, and C. Monroe, Nature Physics **12**, 907 (2016).
[11] J.-y. Choi, S. Hild, J. Zeiher, P. Schauß, A. Rubio-Abadal, T. Yefsah, V. Khemani, D. A. Huse, I. Bloch, and C. Gross, Science **352**, 1547 (2016).
[12] P. Bordia, H. P. Lüschen, S. S. Hodgman, M. Schreiber, I. Bloch, and U. Schneider, Phys. Rev. Lett. **116**, 140401 (2016).
[13] E. Altman and R. Vosk, Annual Review of Condensed Matter Physics **6**, 383 (2015).
[14] R. Nandkishore and D. A. Huse, Annual Review of Condensed Matter Physics **6**, 15 (2015).
[15] D. Porras and J. I. Cirac, Phys. Rev. Lett. **92**, 207901 (2004).
[16] Y.-L. Wu and S. Das Sarma, Phys. Rev. A **93**, 022332 (2016).
[17] U. Schollwck, Annals of Physics **326**, 96 (2011).
[18] P. Hauke and M. Heyl, Phys. Rev. B **92**, 134204 (2015).
[19] R. Hanson, L. P. Kouwenhoven, J. R. Petta, S. Tarucha, and L. M. K. Vandersypen, Rev. Mod. Phys. **79**, 1217 (2007).
[20] D. Loss and D. P. DiVincenzo, Phys. Rev. A **57**, 120 (1998).
[21] C. A. Stafford and S. Das Sarma, Phys. Rev. Lett. **72**, 3590 (1994).
[22] X. Hu and S. Das Sarma, Phys. Rev. A **61**, 062301 (2000).
[23] V. W. Scarola and S. Das Sarma, Phys. Rev. A **71**, 032340 (2005).
[24] E. Barnes, D.-L. Deng, R. E. Throckmorton, Y.-L. Wu, and S. Das Sarma, Phys. Rev. B **93**, 085420 (2016).
[25] O. E. Dial, M. D. Shulman, S. P. Harvey, H. Bluhm, V. Umansky, and A. Yacoby, Phys. Rev. Lett. **110**, 146804 (2013).
[26] J. H. Bardarson, F. Pollmann, and J. E. Moore, Phys. Rev. Lett. **109**, 017202 (2012).
[27] B. Bauer and C. Nayak, Journal of Statistical Mechanics: Theory and Experiment **2013**, P09005 (2013).
[28] S. Iyer, V. Oganesyan, G. Refael, and D. A. Huse, Phys. Rev. B **87**, 134202 (2013).
[29] D.-L. Deng, J. H. Pixley, X. Li, and S. Das Sarma, Phys. Rev. B **92**, 220201 (2015).
[30] D.-L. Deng, X. Li, J. H. Pixley, Y.-L. Wu, and S. Das Sarma, ArXiv e-prints (2016), arXiv:1607.08611 [cond-mat.dis-nn].
[31] X. Li, D.-L. Deng, Y.-L. Wu, and S. Das Sarma, ArXiv e-prints (2016), arXiv:1609.01288 [cond-mat.stat-mech].
[32] S. Aubry and G. André, Ann. Israel Phys. Soc **3**, 18 (1980).
[33] M. Y. Azbel, J. Exptl. Theoret. Phys. (U.S.S.R.) **46**, 929 (1964).
[34] P. G. Harper, Proceedings of the Physical Society. Section A **68**, 874 (1955).
[35] D. R. Grempel, S. Fishman, and R. E. Prange, Phys. Rev. Lett. **49**, 833 (1982).
[36] X. Li, S. Ganeshan, J. H. Pixley, and S. Das Sarma, Phys. Rev. Lett. **115**, 186601 (2015).
[37] R. Modak and S. Mukerjee, Phys. Rev. Lett. **115**, 230401 (2015).